JOURNAL OF APPLIED ELECTROCHEMISTRY 12 (1982) 735–742

The effect of electrolytically formed gas bubbles on ionic mass transfer at a plane vertical electrode

C. I. ELSNER, S. L. MARCHIANO

Instituto de Investigaciones Fisicoquímicas Teóricas y Aplicadas, (INIFTA), Casilla de Correo 16, Suc. 4. (1900) La Plata, Argentina

Received 23 February 1982

The mechanism which explains the increase in the rate of mass transfer through bubble evolution is not completely established. Three models have been proposed. The present work reports experimental results obtained with a cell design which can separate the contribution of the parameters defining each model.

The results obtained allow one to conclude that the main contribution to the increase in the mass transfer rate is due to the macroscopic motion of the fluid caused by the ascending bubbles. A competition between the size and the number of the bubbles at different current densities would be the cause of the constant mass transfer current over a range of gas evolution rates.

Nomenclature

I_g	total constant current applied to the generator electrode (mA)
I_i	current related to the electrochemical gas evolution (mA)
I_m	mass transport current (mA)
j_g	total constant current density ($mAcm^{-2}$)
j_i	gas evolution current density ($mAcm^{-2}$)
j_{H_2}	hydrogen evolution current density ($mAcm^{-2}$)
$j_{i,m}$	mass transfer current density for the i electrode ($mAcm^{-2}$)
j_m	mass transfer current density ($mAcm^{-2}$)
j_l	free convection limiting current density ($mAcm^{-2}$)
x	the distance from the origin of the hydrogen boundary layer to the test electrode (mm)
h_1	height of the generator electrode (mm)
h_2	height of the inert gap between electrodes (mm)
h_i	height of the n electrodes (mm)
h	height of the single electrode (mm)
a	electrode width (mm)
δ	diffusional boundary layer thickness (cm)
Δj_{im}	difference between j_{im}.

1. Introduction

Many electrochemical reactions which are particularly interesting from the technological standpoint, occur with the simultaneous evolution of a gas in a parallel electrode reaction. Usually, this type of process implies the formation of bubbles which changes drastically the hydrodynamic conditions in the solution. Consequently, the mass transfer rate is modified according to the rate and conditions of bubble formation.

The mechanism which explains the change in the rate of mass transfer through bubble evolution is not completely established. For this purpose three models have been proposed, namely the penetration, the hydrodynamic and the microconvective models [1–3].

The penetration model [1, 4–6] considers that a bubble leaving the electrode surface generates an empty space which is filled with fresh solution flowing from the bulk of the solution to the electrode. During this process the diffusional boundary layer is destroyed and the mass transfer process is therefore accelerated. Afterwards, the diffusional boundary layer is reestablished and a new bubble begins to grow. The formation of the

0021–891X/82/060735–08$03.46/0

new bubble decreases the rate of the electrochemical process. Hence, in the penetration model the successive formation and detachment of bubbles produce a periodic variation in the rate of mass transfer.

According to the hydrodynamic model [2, 7, 8] the ascending bubbles provoke the motion of the surrounding fluid and induce a hydrodynamic flow along the electrode which simultaneously increases the mass transfer rate towards the electrode surface.

The microconvective model [3, 9] describes the effect in terms of the growing bubble adhering to the electrode surface. The liquid around the bubble is pushed away radially. This microconvective flow which is developed in the vicinity of the bubbles is damped as the distance to the bubble centre is increased.

Unfortunately none of the three models briefly described above, give a full account of the experimental findings on the influence of bubble stirring in electrochemical processes.

Another possibility is to consider a combined physical model involving the ideas of both the penetration and the hydrodynamics models. On the basis of this idea, the present work reports experimental results obtained with a cell design which allows, in principle, the separation of the contribution of the parameters defining each model. To understand the basic principles related to the influence of bubbles on electrode processes occurring at a vertical plane electrode, a cell geometry, is used where natural convection is relatively well defined.

2. Experimental procedure

Essentially two types of experimental approaches were followed. The first one was similar to that described in recent papers [1–7], and for this purpose a two compartment electrolysis cell, Fig. 1, was used. The electrode compartments were separated by two fritted glass discs (porosity number 4), to avoid the passage of ions from one compartment to the other, at least during each run.

The working electrode consisted of a 99.99% Pt plate vertically mounted in an acrylic holder. The working electrode piece was covered with an acrylic bell-shaped lid for collecting the gases produced during the electrolysis (Fig. 2a).

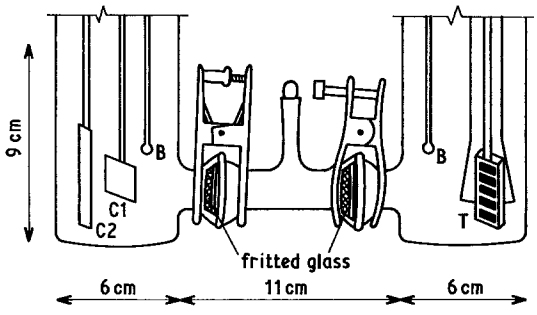

Fig. 1. Diagram of the cell. T, working electrode; C1, counter-electrode at constant potential; C2, counter-electrode at constant current; B, gas bubbler.

The working electrode, the reference electrode and a gas bubbler were placed into one compartment and the counterelectrode and another gas bubbler were placed in the other compartment.

1 mol dm^{-3} sodium hydroxide with 0.03 mol dm^{-3} potassium ferricyanide was used as the electrolyte. This was deaerated with purified nitrogen and before each run it was saturated with the gas whose bubbles were formed during the electrolysis.

The working electrode was maintained under a constant current (I_g) at which the gas evolution reaction and the redox-test reaction took place simultaneously, the latter being under mass transfer control. The total current, I_g, was then the sum of the current related to the electrochemical formation of bubbles I_i (i = H_2 or O_2) and the current related to the mass transfer process, I_m.

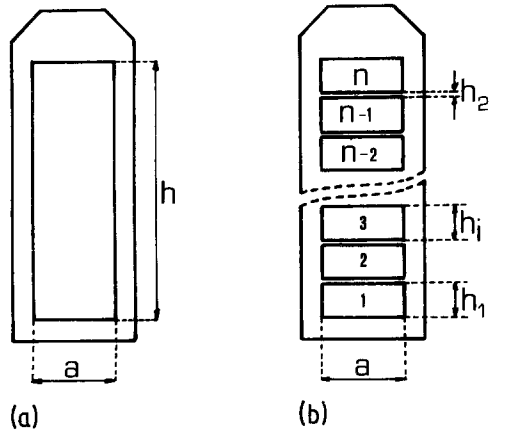

Fig. 2. Schemes of the different electrodes. (a) single electrode, (b) sectioned electrode. a = 1 cm; h_2 = 0.01–0.1 cm; h_i = 0.4 cm; h_1 = 0.2–1.5 cm; h = 3 cm.

Table 1. Electrode characteristics. Counter electrode area = 8 cm² (See Fig. 2)

Number of electrodes	*Material*	h_1 (cm)	h_2 (cm)	h_i (cm)	a (cm)
1	Pt	3.2	–	–	1.05
4	Pt	1.4	0.1	0.39	0.93
4	Ni	1.5	0.1	0.4	1.00
7	Ni	0.2	0.01	0.4	1.00
12	Ni	0.2	0.01	0.4	1.00
7	Pt	0.2	0.01	0.4	1.00

I_i was evaluated from gas volume measurements, and I_m was calculated from the change of concentration of the ferricyanide produced during the electrolysis, by conventional analytical techniques.

The second type of experiments were carried out with a working electrode made from Ni or Pt plates mounted on an araldite holder, which was divided into several independent sections (Fig. 2b). The dimensions as well as the material of the different working electrodes used are given in Table 1. The cell design was essentially the same as that already described, except the cell compartment separation and the use of a second counterelectrode.

The electrolyte solutions were either 1 mol dm^{-3} NaOH with 0.03 mol dm^{-3} potassium ferrocyanide and 0.03 mol dm^{-3} potassium ferricyanide or 1 mol dm^{-3} H_2SO_4 with 0.035 mol dm^{-3} ceric sulfate as a test reagent.

In these runs galvanostatic and potentiostatic techniques were simultaneously used for the different sections of the working electrode. For this purpose a suitable electronic device was made (Fig. 3). One electrode section (generator electrode) was held under a constant current density, j_g, in the 10 to 1000 mA cm^{-2} range. The generator electrode behaved as in the first type of experiments. The remaining electrode sections (test electrodes) were held at a constant potential in the potential range related to the limiting current of the indicator reaction, avoiding the gas evolution reaction. The current at each indicator electrode was independently recorded. In some experiments either all the indicator electrodes or a couple of them were held at the same constant potential.

Different reference electrodes were used, accordingly to the indicator reactions, namely, saturated calomel electrode, Hg/HgO electrode, ferrocyanide/ferricyanide/Pt and $Ce^{3+}/Ce^{4+}/Pt$. Runs were made at temperatures between 25 to 30 ± 0.05° C.

Before each run the working electrode surface was mirror polished with emery paper and an alumina suspension (0.3 μm average diameter) and then activated following the usual procedure. The counterelectrode was a platinum sheet of 8 cm^2 of area.

The steady state current density was read for each working electrode. The i_l versus $x^{1/4}$ relationship was confirmed with the sectioned test electrodes.

3. Results

Results obtained in the first series of experiments are plotted as j_m and j_i versus j_g (Fig. 4).

Curves 1 and 2 correspond to hydrogen evolution j_{H_2} and to the mass transfer indicator reaction, j_m, respectively, plotted as a function of the total constant current j_g.

For j_g values between 0 and 5 mA cm^{-2} a

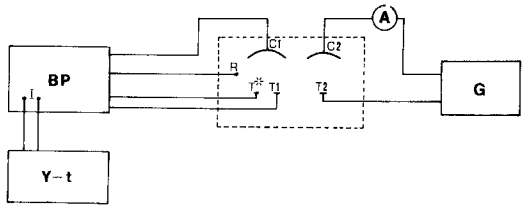

Fig. 3. Diagram of the circuit employed with the sectioned electrode cell. A, ammeter; BP, bipotentiostat; Y-t, recorder; G, galvanostat; R, reference; T*, T1, working electrodes at constant potential; C1 counterelectrode at constant potential; T2 working electrode at constant current; C2 counterelectrode at constant current.

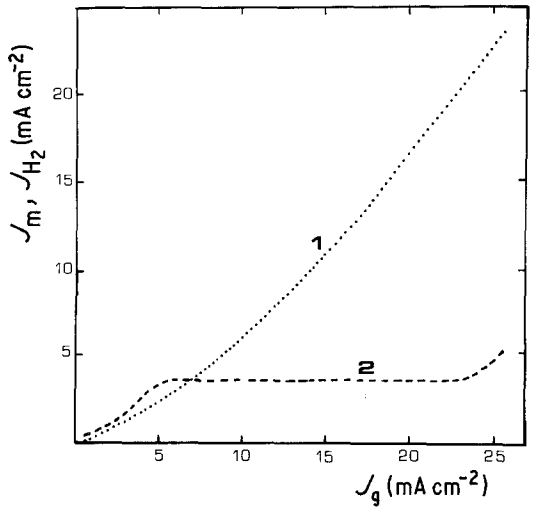

Fig. 4. Dependence of j_m and j_{H_2} on the applied total current density, j_g. ...., Curve 1 hydrogen evolution reaction; – – –. Curve 2 test mass transfer control reaction (ferricyanide ion reduction).

smooth increase of the mass transfer current density j_m is observed. When j_g is greater than 6 mA cm^{-2}, j_m reaches a constant value, six times greater than that corresponding to natural convection, j_l, while j_{H_2} continues to increase.

Finally when the value of j_g exceeds about 24 mA cm^{-2}, j_m increases again. These results which confirm previous findings [1–7] are replotted in the way usually given in the literature by plotting the diffusion boundary layer thickness δ against the gas current density j_i (Fig. 5).

However, the results obtained with this type of experiment are not suitable for testing the different models for interpreting the contributions made to the stirring produced by bubbles in electrochemical reactions. A second type of experiment was therefore attempted.

In these, before each series of runs, the continuity of the hydrodynamic and diffusional boundary layers, was tested. In this case, a linear relationship between j_l and the 1/4th power of the distance from the origin of the hydrodynamic boundary layer should be obtained, when either single undivided or sectionally divided electrodes (with very thin gaps between sections) are held at the same potential, and the mass transfer process is under natural convection.

Once the continuity of the hydrodynamics and diffusional boundary layer was tested, the generator electrode was held under a constant current in the gas evolution region, while the test electrode was maintained at a constant potential. The limiting current density for the redox test reaction was then recorded and the results were plotted as j_m versus j_g (Figs 6–8). In all the cases the bubbles were produced at the bottom electrode and the limiting current density was recorded for the electrodes above. The stirring effect produced at the different sections by the hydrogen gas bubbles and hence the limiting current density changes with the position of the working electrode section (Fig. 6). The same effect is produced by oxygen gas bubbles on the ferrocyanide ion electro-oxidation (Fig. 7) as well as on the ferricyanide ion electroreduction (Fig. 8). As j_g increases, j_m increases relatively fast when j_g is slightly greater than j_l. Afterwards, a j_g range is reached where j_m becomes practically constant. The greatest increase of j_m corresponds to the electrode section located immediately above the generating electrode, where a maximum j_m value

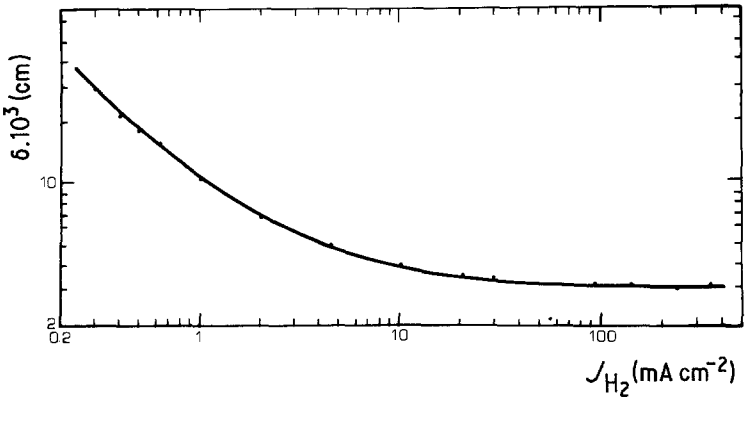

Fig. 5. Diffusion boundary layer thickness, δ, versus the hydrogen evolution current density, j_{H_2}, in a single electrode cell.

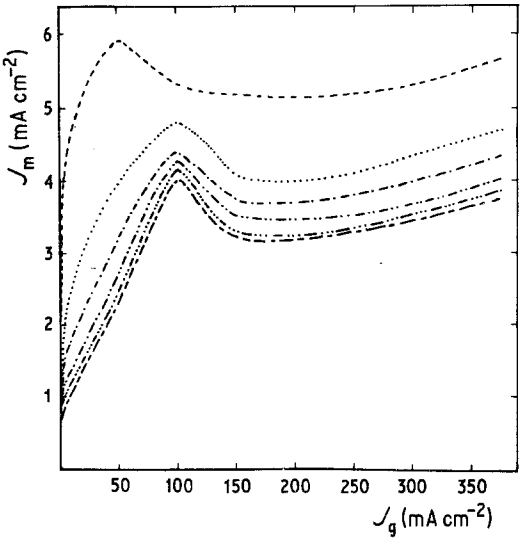

Fig. 6. j_m at the test electrodes versus j_g at electrode 1 (hydrogen evolution and ferricyanide ion reduction reactions). ——, electrode 2; ···, electrode 3; —·—, electrode 4; – – ··, electrode 5; —···—···, electrode 6; – – –, electrode 7.

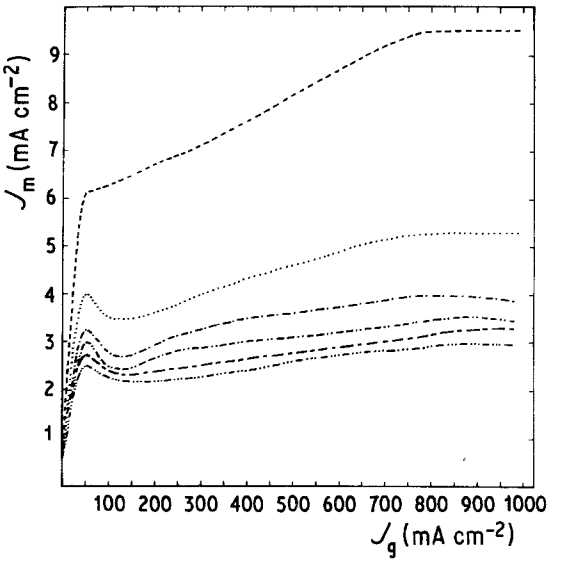

Fig. 8. j_m at the testing electrodes versus j_g at electrode 1 (oxygen evolution and ferricyanide reduction reactions). ——, electrode 2; ···, electrode 3; —·—·—, electrode 4; —·—···—, electrode 5, ——, electrode 6; —···—···, electrode 7.

is observed when j_g is approximately 50 mA cm^{-2}. For the other sections the maximum value results when j_g is 100 mA cm^{-2}.

The greatest j_m corresponds to the ferricyanide ion electroreduction under stirring by hydrogen bubbles. On the other hand, for the oxidation of ferrocyanide and when oxygen is produced at the generator electrode, the increase in j_m observed at the lowest indicator electrode is greater than that for hydrogen bubbles evolution. In this case, for the other electrodes, the j_m values are nearly the same as for the ferrocyanide ion test reaction under the oxygen bubbles stirring.

A comparison of the relationship between j_m and x resulting from these experiments and those obtained for natural and forced convection is relevant. The experimental relationship obtained when bubbles are evolved (Fig. 9) is: $j_m = f(x^{-a})$, $0 \leqslant a \leqslant 1/3$.

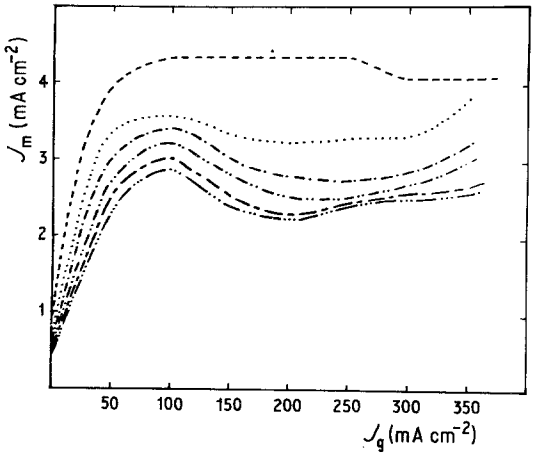

Fig. 7. j_m at the testing electrodes versus j_g at electrode 1 (oxygen evolution and ferrocyanide oxidation reactions). ——, electrode 2; ···, electrode 3; —·—·—, electrode 4; —·—···—, electrode 5; ——, electrode 6; —···—···, electrode 7.

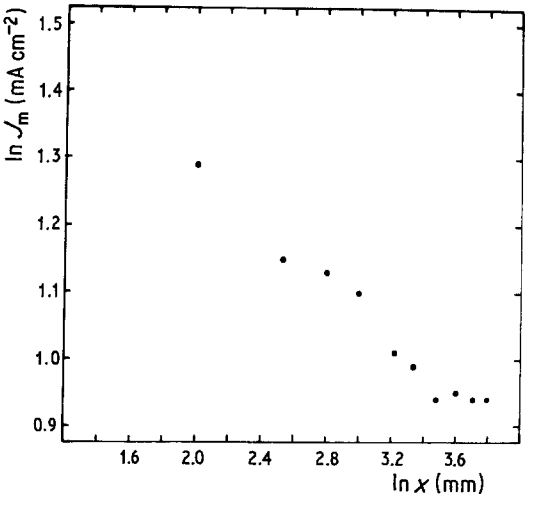

Fig. 9. j_m versus x logarithmic plot.

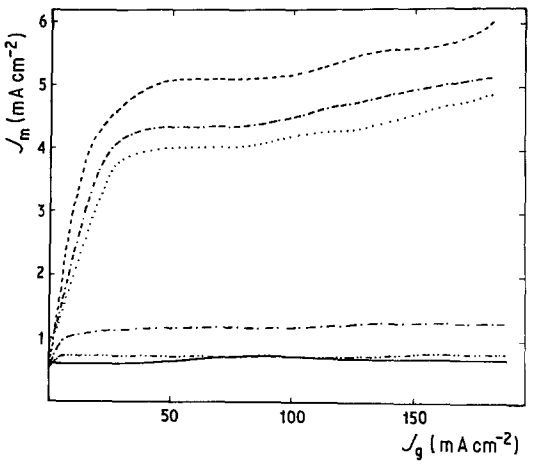

Fig. 10. j_m at the test electrodes versus j_g at electrode 4 (hydrogen evolution and ferricyanide ion reduction reactions). –, electrode 1; –··–, electrode 2; –·–·–, electrode 3; ––––, electrode 5; ––·––, electrode 6; ···, electrode 7.

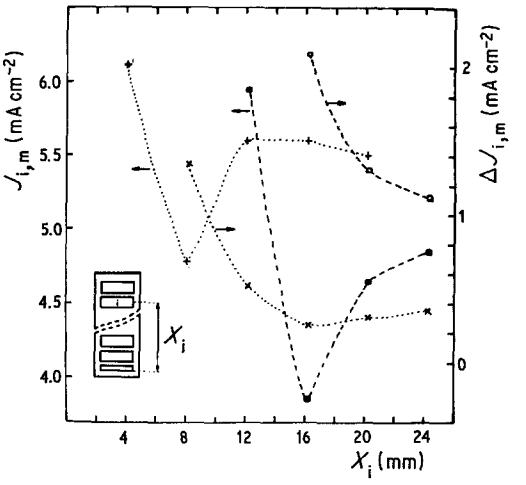

Fig. 11. Plots of j_m and Δj_m versus x for a pair of test electrodes. ··· electrode pairs formed with electrode 2 and electrodes 3–6. – – – pairs formed with electrode 4 and electrodes 5–7.

When one of the central sections of the working electrodes is used as the generator an increase of j_m in the upper electrode is observed (Fig. 10). Conversely, the j_m values of the electrodes located below the generator electrode are only slightly greater than j_l (limiting current density under free convection). In this case a remarkable influence is found only at the electrode located immediately below the generator electrode, where j_m is about twice the j_l value.

Another type of measurement was made using the lowest section of the working electrode as a generator electrode and two of the remaining sectioned electrodes were employed as test electrodes. The latter were maintained at the same constant potential.

All possible combinations of n different electrodes taken two at a time were tested. I_m values were simultaneously recorded for both electrodes on an x, y_1, y_2 recorder.

In this case, for each electrode, the j_m versus j_g relationship was similar to that obtained in the experiments already described, when all the electrodes were held at a constant potential. But the relationship between j_m and x depends in a complex way on the location of the test electrodes with respect to the generator electrode as well as the gap between the two test electrodes. Thus, the first electrode held at a constant potential exhibits the highest mass transfer limiting current density; the next one shows a sudden decrease of j_m but the latter, for the more distant electrodes, increases again asymtotically reaching a constant value (Fig. 11).

Then when the gap between the two electrodes held at a constant potential is large enough, the same $j_{i,m}$ as that corresponding to a single electrode held at a constant potential is observed. For the latter, j_m decreases with x, at a rate which depends on the distance between the test and the generator electrode (Fig. 12).

4. Discussion

Two main conclusions are derived from the experimental results: firstly the differences in j_m when

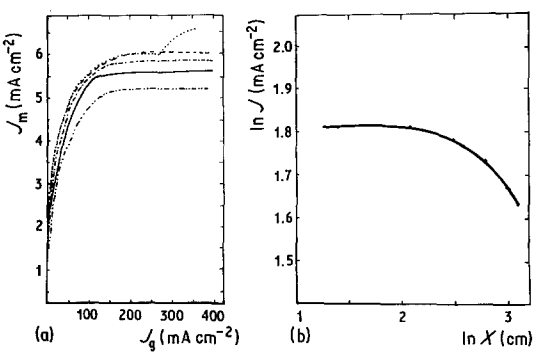

Fig. 12. (a) Plots of j_m for each test electrode versus j_g at electrode 1; ···, electrode 2; – – –, electrode 3; – · –, electrode 4; ——, electrode 5; – ·· – electrode 6. (b) Logarithmic plot of j_m versus x. Data taken from plot 11.

the generator electrode and the test electrodes are placed in the same position is small and secondly the existence of the plateau in the j_m versus j_g plot (Figs 4, 6–8, 10, 12a) is independent whether it is the generator or the test electrode. These facts suggest that the increase of mass transfer rate produced by the electrochemically formed bubbles is mainly due to the hydrodynamic effect.

Let us then suppose that the effect shown in Figs 6–8 depends on the rate of the gas production. This quantity is reflected either by the number of bubbles or by their sizes. These two variables determine the flux velocity produced by the ascending bubbles at the particular j_g value. When j_g is small, but greater than j_l an increase of j_g should produce an increase in the number of bubbles. When a large j_g value is attained, a further increase of j_g increases the amount of gas and the number of bubbles but their size either remains constant or is diminished [10]. For these reasons the ascending rate of each bubble is diminished [11] and the two effects are counter-balanced. If the amount of gas increases again, the diameter of the bubbles also increases due to more gas forming and/or by the coalescence of the neighbouring bubbles either on the electrode or in the bulk of the electrolyte.

When one of the central sections of the electrode is used as the generator electrode, the difference in j_m values of the upper and the lower electrodes also indicates that, in the current density range used in these experiments, the increase of j_m is mainly caused by the ascending motion of the bubbles. Under these circumstances the small influence of bubbles on j_m at the lower electrodes may be related to either the back effect of the fluid flow, which results from the electrolyte flux in the neighbourhood of the generating electrode, or to the penetration effect acting in both directions parallel to the electrode surface. The penetration effect in the upper electrode is added to the hydrodynamic effect.

It is important to take into account the relationship between j_m and x and to compare it with that obtained for natural and forced convection [11]. For natural convection the relationship holding for the present cell design is $j_m = f(x^{-1/4})$ and for the forced convection it is $j_m = f(x^{-1/2})$. The type of relationship obtained when all the upper working electrode sections are held at the same potential and the bubbles are evolved at the generator electrode is $j_m = f(x^{-a})$ but the exponent of x is between 0 and 1/3. The exponent a decreases as x increases.

When only one section of the working electrode is kept at a constant potential, the current at the test electrodes nearest to the generator electrode becomes independent of x, and afterwards it falls abruptly as x increases (Fig. 12).

For natural convection the motion of the electrolyte occurs inside the hydrodynamic boundary layer thickness, but for forced convection the bulk of the fluid is in motion and a greater dependence of j_m on x is observed.

When electrolytically produced bubbles are present, the ascending motion is associated with a flux of electrolyte solution. Hence the influence of bubbles should be confined to a region of about the same order of magnitude as the radius of the bubbles and smaller than the hydrodynamic boundary layer thickness. On the other hand, when an electrode section above and far from the generator electrode is considered, the bubbles in their upward motion are appreciably separated from the electrode surface and their stirring effect diminishes. This interpretation agrees with the findings of other authors, where the exponents of x are smaller than 1/4.

When the bubble formation and the indicator ion electrochemical reaction occur simultaneously on the same electrode, bubbles are detached from the whole surface, acting consequently always in the inner part of the hydrodynamic boundary layer. In this case, the exponent would be smaller and near 0.

The results obtained with a pair of test electrodes held at the same potential also support the same physical mechanism for interpreting bubble stirring.

This series of experiments reveals that the tangential and perpendicular mass transport are very important in the diffusion boundary layer.

The sudden decrease of j_m in the nearest neighbouring test electrode, may be explained on the basis of the depletion of the test ion in the diffusion boundary layer at the lower electrode of the electrode pair so the transport contribution occurs principally in the direction normal to the surface and hence the current density decreases.

The presence of an inert gap, where the reaction is inhibited changes the diffusion conditions. In this case the test ions diffuse from a non depleted solution in the normal as well as in the tangential directions.

As the gap between the connected electrodes increases, the fluid streaming past the upper electrode is not depleted in the reacting species and the current density increases again. But the values of j_m never reach those of the first electrode because the bubbles are more distant from the working electrode surface during their ascending motion and their influence obviously diminishes. Therefore, the results shown in Fig. 10 can be qualitatively explained.

5. Conclusions

It can be concluded that:

1. The main contribution to the increase in the rate of the convective diffusion controlled electrochemical process due to bubble formation should be assigned to the macroscopic motion of the fluid caused by the ascending bubbles.

2. Under the considered experimental conditions there was a minor contribution of the penetration mechanism. This contribution increases as j_g increases.

3. The tangential mass transport is relevant, its contribution being of the same order of magnitude as that of the perpendicular mass transport contribution.

Acknowledgements

INIFTA is sponsored by the Consejo Nacional de Investigaciones Científicas y Técnicas (CONICET), the Comisión de Investigaciones Científicas de la Provincia de Buenos Aires (CIC) and the Universidad Nacional de La Plata. Ing. C.I.E. would like to thank CONICET for the fellowship grant. The authors are indebted to Professor A. J. Arvía for valuable discussion and suggestions.

References

[1] N. Ibl and J. Venczel, *Metalloberfläche* **24** (1970) 365.
[2] L. J. J. Janssen and J. G. Hoogland, *Electrochim. Acta* **15** (1970) 1013.
[3] H. Vogt, *Fortschritte der Verfahrenstechnik, D* **16** (1978) 297–332.
[4] N. Ibl, *Chemie Ing. Techn.* **35** (1963) 353.
[5] J. Venczel, *Electrochim. Acta* **15** (1970) 1909.
[6] N. Ibl, E. Adam, J. Venczel and E. Schlach, *Chem. Ing. Techn.* **43** (1971) 202.
[7] L. J. J. Janssen and J. G. Hoogland, *Electrochim. Acta* **18** (1973) 543.
[8] L. J. J. Janssen, *Electrochim. Acta* **23** (1978) 81.
[9] H. Vogt, *Electrochim. Acta* **23** (1978) 1019.
[10] B. Kabanov and A. Frumkin, *Z. Phys. Chem.* **165** (1933) 433.
[11] V. Levich, 'Physicochemical Hydrodynamics', Prentice Hall, Englewood Cliffs, New Jersey (1962).